The relaxation behaviour of supersaturated iron in single-crystal silicon at 500 to 750°C

J. D. Murphy and R. J. Falster

Citation: J. Appl. Phys. **112**, 113506 (2012); doi: 10.1063/1.4767378
View online: http://dx.doi.org/10.1063/1.4767378
View Table of Contents: http://jap.aip.org/resource/1/JAPIAU/v112/i11
Published by the American Institute of Physics.

The relaxation behaviour of supersaturated iron in single-crystal silicon at 500 to 750 °C

J. D. Murphy[1,a)] and R. J. Falster[1,2,b)]
[1]*Department of Materials, University of Oxford, Parks Road, Oxford OX1 3PH, United Kingdom*
[2]*MEMC Electronic Materials, viale Gherzi 31, 28100 Novara, Italy*

(Received 28 June 2012; accepted 26 October 2012; published online 4 December 2012)

Iron-related defects cause major problems in silicon for both microelectronic devices and photovoltaics. Iron contamination can occur during high temperature processing or, particularly in the case of low-cost photovoltaics, from the feedstock. In many situations, silicon is cooled too rapidly for the establishment of equilibrium, and so the bulk iron concentration exceeds the solubility value. We have investigated the relaxation of supersaturated bulk iron to the equilibrium solubility in single-crystal silicon. Bulk iron concentrations are measured by analysing the change in minority carrier lifetime that occurs when iron-boron pairs are dissociated. High-purity silicon is rubbed with iron and annealed at 750 °C for 24 h. This process creates an iron silicide phase on the rubbed surface and allows the equilibrium solubility of $\sim 2 \times 10^{12}\,\mathrm{cm}^{-3}$ to be established. Samples are then annealed at lower temperatures (500 to 700 °C) for a range of times. The rate of decay in iron concentration depends upon whether a silicide was formed on one side or two sides, with the kinetics in excellent agreement with iron diffusion to one or both surfaces, respectively. Even for the highest supersaturation (~2000 times the solubility), the pre-existence of a silicide on one surface means there is insufficient driving force for nucleation of a silicide on the other surface. Relaxation experiments were also performed on contaminated samples for which the iron silicide source at the surface was removed after contamination. The iron concentration decays substantially more slowly in these specimens. The kinetics can be explained by relaxation to bulk voids. © *2012 American Institute of Physics*. [http://dx.doi.org/10.1063/1.4767378]

I. INTRODUCTION

Metallic impurities have deleterious effects in silicon, including ruining microelectronic devices[1] and lowering the efficiency of photovoltaics.[2,3] It is widely recognised that iron is one of the most harmful contaminants.[4] Gettering processes[5] are routinely used to remove iron from active regions of the material, and processes used include gettering to oxide precipitates[6] or porous silicon layers,[7] phosphorus-diffusion gettering,[8,9] boron-diffusion gettering,[8,9] and aluminium gettering.[9,10] Iron can be gettered very effectively in single-crystal silicon,[9] but in multicrystalline silicon (mc-Si), it interacts with extended defects which limits the efficacy of the gettering procedure. In mc-Si, it has been shown that iron decorates dislocations[11] and grain boundaries[12] thus increasing their recombination activity, and that iron forms precipitates which cannot easily be gettered.[13]

Gettering processes are controlled by both kinetic and thermodynamic factors. The diffusion of interstitial iron (Fe_i) in silicon is generally well understood, and Istratov *et al*. have consolidated the results of many studies into the following expression:[14]

$$D_{Fe_i} = \left(1.0\,^{+0.8}_{-0.4}\right) \times 10^{-3} \exp\left(-\frac{0.67\mathrm{eV}}{kT}\right) \mathrm{cm}^2\,\mathrm{s}^{-1}. \quad (1)$$

It is noted that Eq. (1) is based upon data for high temperatures (700 °C to 1265 °C) and low temperatures (0 °C to 400 °C), as data were not available in the intermediate range. An important thermodynamic parameter for gettering is the equilibrium solubility. In the same review,[14] Istratov *et al*. combined many studies at 800 °C to 1200 °C to give the equilibrium solubility of iron in intrinsic silicon as

$$S_{800\rightarrow1200\,^\circ\mathrm{C}} = 8.4 \times 10^{25} \exp\left(-\frac{2.86\mathrm{eV}}{kT}\right) \mathrm{cm}^{-3}. \quad (2)$$

Below 800 °C, there is a growing body of evidence to suggest that more iron can dissolve in low-doped silicon than predicted by Eq. (2). This should not be confused with the well-understood Fermi level effect that gives rise to enhanced iron solubility in highly doped material.[15] In low-doped material, iron's solubility has been measured to be $\sim 1.5 \times 10^{12}\,\mathrm{cm}^{-3}$ at 700 °C by Shabani *et al*.,[16] $4 \times 10^{11}\,\mathrm{cm}^{-3}$ at 670 °C by Aoki *et al*.,[17] up to $\sim 10^{12}\,\mathrm{cm}^{-3}$ at 650 °C by Falster and Borionetti,[18] and $\sim 5 \times 10^{11}\,\mathrm{cm}^{-3}$ at 600 °C also by Shabani *et al*.[16] These measurements are larger than predicted by Eq. (2) by factors of ~12, ~9, up to ~49, and ~193, respectively. In our recent work, we systematically studied the incorporation of iron into silicon, finding the following expression at 600 to 800 °C[19]

$$S_{600\rightarrow800\,^\circ\mathrm{C}} = 1.3 \times 10^{21} \exp\left(-\frac{1.8\mathrm{eV}}{kT}\right) \mathrm{cm}^{-3}. \quad (3)$$

a)john.murphy@materials.ox.ac.uk.
b)rfalster@memc.it.

We also found the iron concentration in samples contaminated below ~600 °C was approximately independent of temperature, with a value of $\sim 8 \times 10^{10}\,\mathrm{cm}^{-3}$. Pre-annealing the sample at higher temperatures gave a lower value of iron concentration, so we suggested that the pre-anneal allowed a different iron silicide phase to form.[19] It has also been suggested that a phase transformation between β-$FeSi_2$ and α-$FeSi_2$ occurs between 760 °C and 920 °C.[20] It is, therefore, possible that the two solubility regimes described by Eqs. (2) and (3) are with respect to a different iron-containing phase, and this is the subject of further investigation.

In boron-doped silicon at low temperatures, positively charged interstitial iron binds to negatively charged substitutional boron to form FeB pairs.[21,22] For moderate boron concentrations (up to $10^{16}\,\mathrm{cm}^{-3}$), the vast majority of FeB pairs dissociate above ~300 °C (Ref. 21) and so interstitial iron is highly mobile (Eq. (1)). Controlling the distribution of iron in mc-Si by optimising thermal processing is necessary to maximise cell efficiency[23,24] and various groups have proposed that long annealing processes at moderate temperatures (300 °C to 600 °C) could improve overall performance by redistributing metallic impurities.[25–27] Although such studies have shown empirical improvements, the precise details of what happens to the supersaturated transition metals are not well understood.

The aim of this paper is to understand the behaviour of supersaturated iron in single-crystal Czochralski silicon (Cz-Si). Understanding such behaviour in the absence of high concentrations of structural defects (such as dislocations and grain boundaries) is the first step in understanding gettering at low temperatures in mc-Si. Samples are first intentionally contaminated with a level of iron corresponding to the equilibrium solubility at 750 °C. They are then annealed at lower temperatures (500 to 700 °C) with iron initially in a supersaturated state. The kinetics of the decay in iron concentration are measured and discussed in terms of iron-containing phases at the surfaces and in the bulk.

II. EXPERIMENTAL METHODS

High-purity boron doped Cz-Si wafers (~2 to ~17 Ω cm) were cleaved into ~5 cm by 5 cm squares. The initial wafer thickness was typically ~700 μm. Samples were rubbed with iron (99.95% purity from Testbourne Limited, UK) on the back (unpolished) side. Some samples were also rubbed on the front (polished) side. All samples were then annealed in air in a pre-heated furnace at 750 °C for 24 h, followed by a rapid cool to room temperature. The samples were cooled to below 200 °C in <10 s. The contamination process creates an iron silicide layer at the rubbed sample surface(s). For some experiments, a total of 30 to 40 μm of material (including the iron silicide layer) was removed from the samples' surfaces using a planar etch comprising HF (40%), HNO_3 (69%), and CH_3COOH (glacial) in the ratio 8:75:17. Samples with and without surface silicide layers were then annealed in air at lower temperatures (500 to 700 °C) for different times, again followed by a rapid cool. After the second anneal, the samples were subjected to an HF dip, followed by an RCA clean. The sample surfaces were then both passivated with silicon nitride grown by direct plasma enhanced chemical vapour deposition at 350 °C.

Minority carrier lifetime was measured at room temperature by quasi-steady-state photoconductance (QSS-PC)[28] using a Sinton WCT-120 lifetime tester. Before testing, samples were placed on a hotplate at 200 °C for 10 min to eliminate any effects related to boron–oxygen defects.[29] To dissociate FeB pairs, >50 flashes with a ~10 μs decay constant from a Quantum Qpaq-X flash lamp placed very close to the sample were used. An initial lifetime measurement was made immediately. A final lifetime measurement was made at least 24 h later, which for the conditions investigated is sufficient time for complete reassociation of the FeB defect.[22]

Figure 1 shows measured minority carrier lifetime as a function of the excess electron density (Δn) for a typical contaminated sample. One curve is the initial measurement in which the iron was in the interstitial state. The other curve is the final measurement in which FeB pairs had re-formed. The injection-dependences are characteristic of the two defects, showing the typical cross-over at low injection.[30,31] Similar curves were acquired for a wide range of samples processed in a variety of conditions. The two lifetime measurements were used to determine the bulk iron concentration using an approach described in detail in our previous work.[19,32] This uses Shockley-Read-Hall statistics[33,34] using the recombination parameters of Rein and Glunz[31] to determine the iron concentration required to account for a lifetime change at a given injection level (generally $0.2N_A$ in this work, where N_A is the doping level). This technique enables the measurement of bulk iron concentrations to a sensitivity of $\sim 10^{10}\,\mathrm{cm}^{-3}$ or better. It is noted that some of the specimens produced in this work have an iron concentration which is not uniform with depth. In such samples, the measured iron concentration represents the average iron

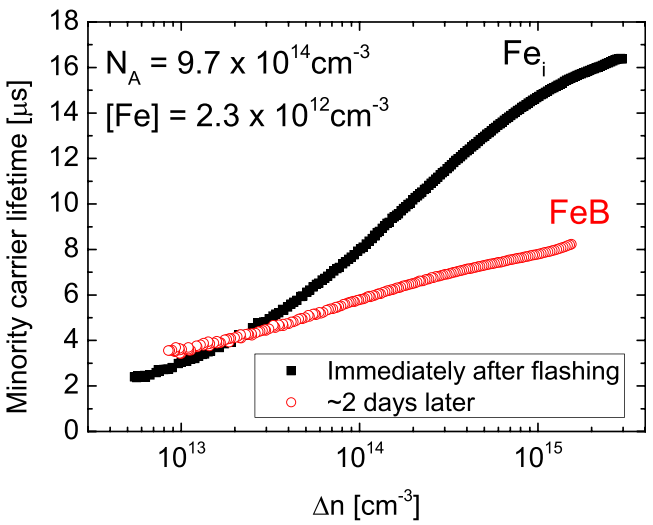

FIG. 1. Minority carrier lifetime versus excess electron density for an iron-contaminated sample immediately after dissociation of FeB pairs and approximately two days later. The example shown is for a sample rubbed with iron on both sides and annealed at 750 °C for 24 h.

concentration in the specimen, provided the carrier generation rate remains approximately uniform throughout the sample.

III. RESULTS AND ANALYSIS

A. Relaxation to surface silicides

A series of experiments was performed to understand the relaxation of supersaturated iron with iron silicide source(s) still present at the surface(s). The iron deposited at the surface by the rubbing process can be considered to be an infinite source for our purposes. One set of high-purity Cz-Si samples was rubbed with iron on the back side only; another set was rubbed on both sides. Both sample sets were then annealed at 750 °C for 24 h to install an initial iron concentration of $\sim 2 \times 10^{12}\,\mathrm{cm}^{-3}$. The samples were not cleaned or etched before being annealed at 650 °C for different times. Figure 2 shows the iron concentration plotted against annealing time at 650 °C. The iron concentration decays to approximately the same value for both sets of samples. The rate of decay is substantially faster for the samples contaminated from both sides.

The kinetics of the relaxation of supersaturated iron were analysed by considering iron diffusion to iron silicide layers at the surfaces. We define the uniform initial iron concentration as $C_{initial}$ and the final uniform concentration as C_{final}. Solving the diffusion equation to both surfaces gives the average iron concentration in the sample, $C_{average}$, at any time, t, to be[35]

$$C_{average} = C_{final} + (C_{initial} - C_{final}) \sum_{\substack{k=1 \\ \text{kodd}}}^{\infty} \frac{8}{\pi^2 k^2} \exp\left(-\frac{D_{Fe} t \pi^2 k^2}{d^2}\right), \tag{4}$$

where k is an integer, D_{Fe} is the diffusion coefficient of iron, and d is the sample thickness. The case of diffusion to just one surface can be found by replacing d in Eq. (4) with $2d$.

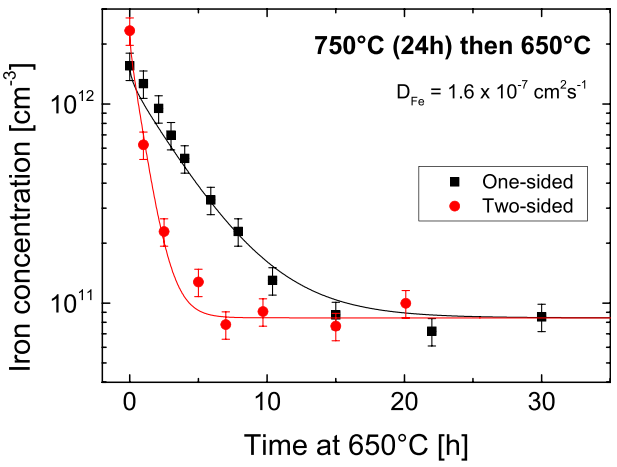

FIG. 2. Iron concentrations measured as a function of time at 650 °C in ~700 μm thick samples pre-contaminated with iron at 750 °C for 24 h. One set of samples was rubbed with iron on the back side; the other was rubbed on both sides. The kinetics of the relaxation are in excellent agreement with iron diffusion to one side or both sides, respectively, with an iron diffusion coefficient of $1.6 \times 10^{-7}\,\mathrm{cm}^2\,\mathrm{s}^{-1}$.

The data in Figure 2 were fitted using Eq. (4). Data for samples contaminated from both sides were fitted according to two-sided diffusion; data for the samples contaminated from just one side were fitted according to one-sided diffusion. Both sets of data could be fitted well with the same diffusion coefficient for iron of $1.4 \times 10^{-7}\,\mathrm{cm}^2\,\mathrm{s}^{-1}$ at 650 °C. This is within the range of values of $1.3 \times 10^{-7}\,\mathrm{cm}^2\,\mathrm{s}^{-1}$ to $4.0 \times 10^{-7}\,\mathrm{cm}^2\,\mathrm{s}^{-1}$ given by Eq. (1) and confirms that the iron concentration reduction occurs by diffusion to pre-existing iron silicide(s) at the sample surface(s).

Samples pre-contaminated by rubbing one side and annealing at 750 °C for 24 h were then annealed at lower temperatures without being cleaned or etched. Figure 3 shows iron concentration relaxation data for such samples annealed at 500 °C to 700 °C for different times. A further set of samples was annealed at 400 °C, but these samples experienced a substantial resistivity change dependent on annealing time. This is attributed to the formation of thermal donor defects[36] and these samples are excluded from the analysis. The value of the final steady-state iron concentration plotted in Figure 3 is dependent on temperature, as is the rate of decay in iron concentration. The data have been fitted using Eq. (4) for a one-sided relaxation by setting the diffusion coefficient for iron to those values shown in the figure. The steady-state final iron concentration at 500 °C and 550 °C lies below our detection limit, so to fit these data we have extrapolated the C_{final} values measured at higher temperatures. Figure 4 is an Arrhenius plot of the iron diffusion coefficient, from which iron diffusivity is deduced to be

$$D_{Fe} = 1.4 \times 10^{-3} \exp\left(-\frac{0.73\mathrm{eV}}{kT}\right) \mathrm{cm}^2\mathrm{s}^{-1}. \tag{5}$$

The error in the activation energy for D_{Fe} is ± 0.05 eV, or alternatively the error in the pre-factor is a factor of ± 3. Equation (5) agrees with the widely used expression for the diffusivity of interstitial iron given by Eq. (1).

B. Relaxation without surface silicides

A further series of experiments was undertaken to understand the relaxation of iron in samples without pre-existing surface silicides. High-purity Cz-Si samples were rubbed with iron on the back side and annealed at 750 °C for 24 h to create a set of specimens with the same starting iron concentration. A planar etch was then used to etch away the iron silicide and some bulk material from the sample surfaces. These specimens without an iron source at the surface were then annealed at lower temperatures. The iron concentrations measured as a function of time are shown in Figure 5. For comparison, data from Figure 3 (for which the iron silicide remained in place on one side) are also plotted.

It is clear from Figure 5 that the rate of decay of iron concentration at all temperatures is substantially slower in the samples from which the surface iron silicide layer has been first removed. The rate of decay is again dependent on temperature. The final value of iron concentration is higher for the silicide-free samples compared to the samples on

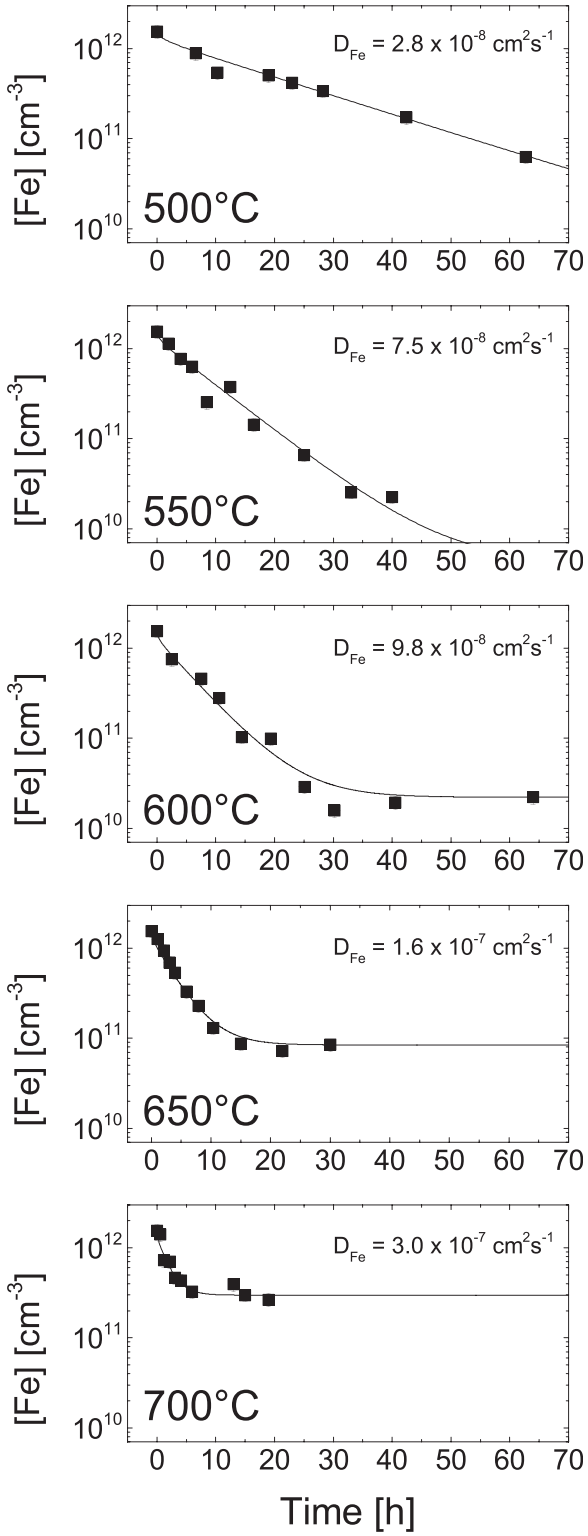

FIG. 3. Average bulk iron concentrations measured after a two-stage thermal process. For all data points, specimens were first contaminated by rubbing one side with iron then annealing at 750 °C for 24 h. Without the removal of the iron-containing surface layer, specimens were then annealed at the temperatures stated for the times plotted. Curves fitted through the data assume iron diffusion to one side according to Eq. (4).

which a silicide layer was retained. There is also more scatter in the data for the silicide-free samples. Possible mechanisms by which the iron concentration decays in the samples without iron silicide surface layers are discussed in Sec. IV B.

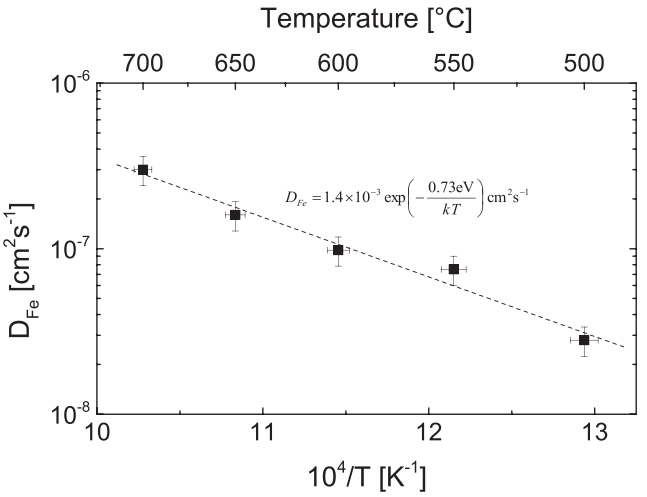

FIG. 4. The diffusion coefficient of interstitial iron deduced from the one-sided iron concentration relaxation data shown in Figure 3.

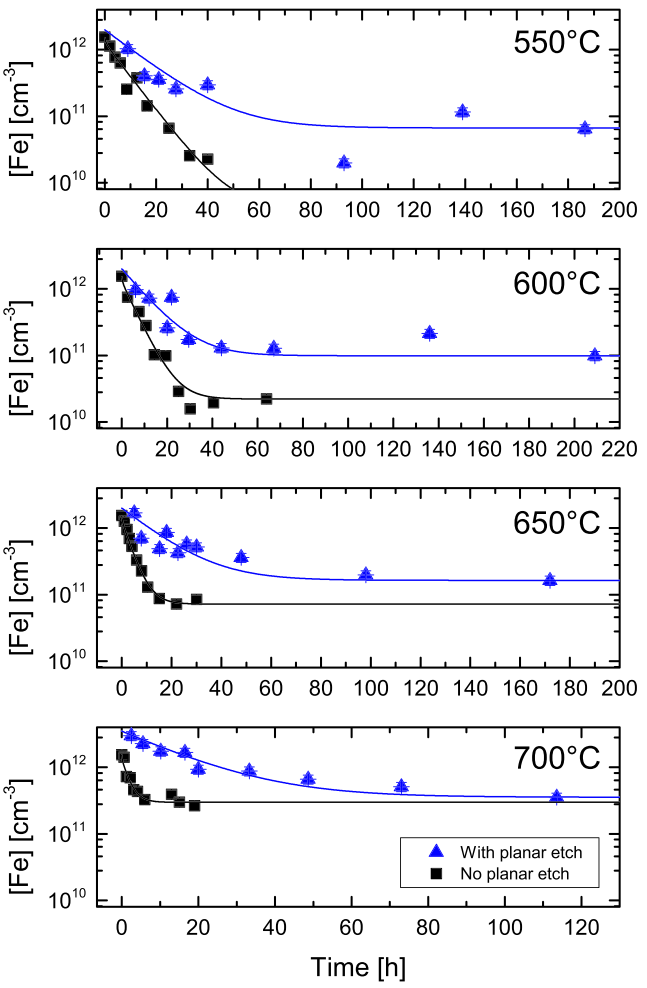

FIG. 5. Average bulk iron concentrations measured after a contamination at 750°C for 24 h followed by an anneal at the temperature shown. Blue triangles denote samples for which the iron silicide source had first been removed by planar etching. For comparison, data from Figure 3 are also shown for samples for which the iron silicide layer remained in place (black squares).

C. Steady-state iron concentrations

The data in Figures 3 and 5 show the iron concentration reaches a steady-state value, where this value is above the

detection limit. Figure 6 is a plot of this steady-state iron concentration versus temperature. Also shown in Figure 6 are (i) data from our previous study using a one-stage thermal treatment on one-side rubbed samples[19] and (ii) a dashed line representing an extrapolation of the established high temperature solubility data given by Eq. (2).[14] Below ~800 °C, data from all three of our different experiment types show a considerable enhancement compared to extrapolation of Eq. (2).

Samples subjected to a 750 °C pre-anneal followed by a lower temperature anneal without silicide removal have a lower final iron concentration than those from our one stage process. For 750 °C pre-annealed samples subsequently annealed at 725 °C and below, the activation energy of the iron concentration is within the experimental error of that given in Eq. (3). Assuming the same activation energy, the steady-state iron concentration varies according to

$$S_{750\,^{\circ}\mathrm{C\,pre-anneal}} = 5.6 \times 10^{20} \exp\left(-\frac{1.8\mathrm{eV}}{kT}\right) \mathrm{cm}^{-3}. \quad (6)$$

The pre-factor in Eq. (6) is therefore ~2.3 times less than that given in Eq. (3). This difference is larger than the random error in the measurement of iron concentrations, which is likely to be less than ~25%. Below ~600 °C, the iron concentration is approximately independent of temperature in the case of a single stage anneal, but it remains temperature-dependent in those samples pre-annealed at 750 °C. Also shown in Figure 6 are the steady-state iron concentrations measured in samples which had their surfaces removed by planar etching. At 700 °C, the value lies between the standard one stage contamination experiment and the 750 °C pre-annealed samples. At 650 °C and 600 °C, the value agrees with the one-stage data published previously.[19] This is discussed in more detail in Sec. IV B.

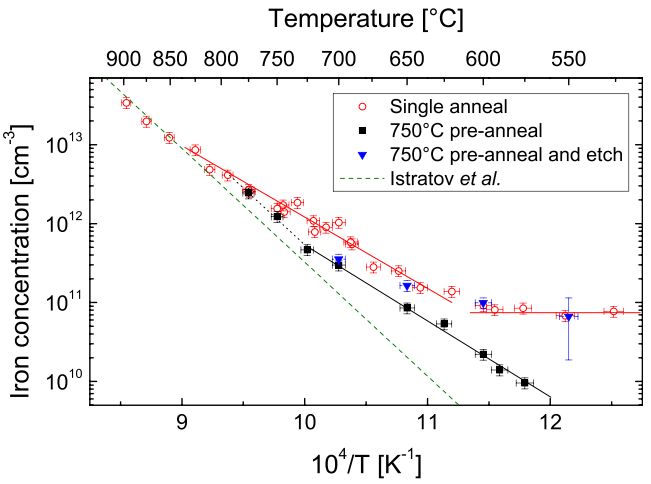

FIG. 6. The concentration of iron in contaminated silicon as a function of contamination temperature. The dashed line represents the well-established high temperature solubility given by Eq. (2). Open symbols denote data from one-stage annealing from our previous work.[19] Closed symbols represent the steady-state concentrations from samples subjected to a pre-anneal at 750 °C (squares) and for samples subjected to a pre-anneal at 750 °C followed by a surface-removal etch.

IV. DISCUSSION

A. Relaxation with pre-existing iron silicide phases

We first consider the relaxation behaviour of iron when the source remains at the sample surface(s), as was the case for data presented in Figures 2 and 3. Figure 2 shows that the kinetics of the decay of supersaturated iron are consistent with iron diffusion to the side(s) initially rubbed with iron. This shows that an iron silicide phase forms at the contaminated side during the 750 °C pre-anneal. We suggest that rubbing the sample with iron has the effect of introducing iron into the bulk, which otherwise may not occur due to the low diffusivity of iron through the native oxide. The supersaturated iron concentration reduces by diffusion to this surface layer upon annealing at lower temperatures (500 to 700 °C). For all these temperatures, the data can be fitted by a one-sided solution of the diffusion equation. The required value of the diffusivity of iron plotted in Figure 4 is in good agreement with the literature data for interstitial iron summarised by Eq. (1). We note that this widely used expression is based on data from high temperatures (>700 °C) and low temperatures (≤400 °C) and not at the temperatures studied here. Equation (5) thus represents a measurement of the diffusivity of interstitial iron in this wide in-between region.

The degree of supersaturation of iron can be quantified in terms of the ratio of the starting iron concentration to the steady-state iron concentration. The pre-anneal at 750 °C introduces $\sim 1.6 \times 10^{12}\,\mathrm{cm}^{-3}$ of bulk iron. The steady-state bulk iron concentrations in our relaxation experiments were $\sim 3.2 \times 10^{11}\,\mathrm{cm}^{-3}$ at 700 °C, $\sim 7.9 \times 10^{10}\,\mathrm{cm}^{-3}$ at 650 °C, and $\sim 2.1 \times 10^{10}\,\mathrm{cm}^{-3}$ at 600 °C. At lower temperatures, the steady-state concentration is below our detection limit, but extrapolation of data in Figure 6 gives estimates of $4.6 \times 10^{9}\,\mathrm{cm}^{-3}$ at 550 °C and $8.0 \times 10^{8}\,\mathrm{cm}^{-3}$ at 500 °C. Thus, for our experiments, the initial supersaturation level of iron relative to the equilibrium value was ~5.0 at 700 °C, ~20 at 650 °C, ~75 at 600 °C, ~350 at 550 °C, and ~2000 at 500 °C. The driving force for nucleation of an additional iron silicide phase would be dependent on the supersaturation. The fact that we can fit our data using one-side diffusion down to 500 °C shows that additional phases have not been formed in our relaxation experiments. We conclude therefore that when an iron silicide phase pre-exists at a sample surface, a supersaturation of ~2000 times or less is insufficient to nucleate additional phases, either at the other surface or in the bulk.

Figure 6 shows the equilibrium iron concentration is dependent upon the thermal history of the samples. The fully relaxed iron concentration in samples pre-annealed at 750 °C with the silicide retained is significantly lower than we find in our one-stage experiment published previously.[19] This difference could be due to differences in the iron-silicide phases formed by the two different thermal treatments. Comparison of Eqs. (3) and (6) suggests that this difference may lie in the solubility pre-factor. Solubility pre-factors are dependent upon entropy differences between phases in equilibrium.[37] Thus, it is possible that the two-stage treatment creates an iron silicide phase which has a different entropy relative to the bulk silicon than in the one-stage case. However, this

explanation is speculative and the structural details of the phases are the subject of further investigation.

B. Relaxation without pre-existing iron silicide surface phases

We now consider the relaxation behaviour of iron when the iron source has been removed from the sample surface. Figure 5 shows the iron concentration reduces much more slowly in these samples than it did when the silicide layer was retained at one side. We offer two possible explanations for the mechanism of iron loss from the bulk in these samples. The first is that iron silicide phases nucleate and grow at both free surfaces. The second is that iron silicide precipitates nucleate at defects in the bulk, such as voids. We discuss each possible explanation in turn.

Creation of iron silicide phases at the surfaces would probably result in a complicated time-dependence in the iron concentration plots, with a diffusion-limited growth stage following a thermodynamically determined nucleation phase. Although there is more scatter in the data for etched samples in Figure 5, the decay is generally quite smooth. From the results presented in Figure 5 alone, it is not possible to establish whether the excess iron is precipitating at the surfaces, but also it is not possible to rule this out.

It is also possible that the excess iron forms iron-containing precipitates in the bulk. Such precipitation would require nucleation sites, but it has previously been shown that metallic precipitates can nucleate at voids[38] which exist in very low concentrations in the high quality material used. If it is assumed that excess iron is lost to uniformly distributed spherical sinks, the bulk iron concentration at $t > 0$ is given by

$$C_{bulk}(t) = C_{initial} - 4\pi RND_{Fe}\sum_{i=0}^{t}(C_i - C_{final}), \qquad (7)$$

where i is an integer, C_i is the bulk iron concentration at the ith time step, R is the sink radius, and N is the sink density. Equation (7) has been used to fit the experimental data for etched samples in Figure 5 and, although there is some scatter in the experimental data, the trends can be matched well. The values of D_{Fe} used in the fitting were those deduced from the data plotted in Figure 4 from the single-sided relaxation experiments. The other fitting parameter is the product of the sink radius and concentration (RN). For the fits shown, RN is $7\,cm^{-2}$ at 700 °C, $11\,cm^{-2}$ at 650 °C, $35\,cm^{-2}$ at 600 °C, and $50\,cm^{-2}$ at 550 °C.

It is not surprising that RN would depend upon the degree of iron supersaturation and this could be explained in two ways. The first possible explanation involves varying N, with the number of voids at which iron precipitation occurs depending on the level of supersaturation. Under this assumption, the number of voids at which iron silicide precipitates nucleate is enhanced compared to the 700 °C value by a factor of 1.6 at 650 °C, 5 at 600 °C, and 7.1 at 550 °C. A void radius of 50 nm therefore requires an active void density of $1.4 \times 10^6\,cm^{-3}$ at 700 °C and $1 \times 10^7\,cm^{-3}$ at 550 °C. This order of magnitude is consistent with the expected void density in modern high quality Cz-Si material. The second possible explanation essentially involves varying R. For small supersaturation levels, iron silicide layers could coat the inside of voids. At larger supersaturations, these precipitates grow into larger needle-shaped defects which would increase the effective value of R. It has long been known that rod-like iron silicides can form in silicon.[39–41]

Figure 5 shows that the steady-state iron concentration reached after relaxation can be different depending on whether or not an iron silicide source was left at the surface. The steady-state iron concentrations for these samples and those subjected to a one-stage process are plotted in Figure 6. The behaviour in the samples in which the source had been removed more closely resembles the one-stage treatment than the two-stage treatment with the source still in place. It is notable that the data points at 550 °C and 600 °C are consistent with the temperature-independent iron concentration regime observed in the one-stage experiments.

V. CONCLUSIONS

We have investigated the behaviour of iron in silicon in the 500 to 750 °C temperature range. In this temperature range, we confirm that iron is distinctly more soluble than expected from established high temperature data. We also confirm that the diffusivity of iron is in agreement with data at higher and lower temperatures. Experiments have been performed to understand the behaviour of supersaturated iron at these temperatures. When the iron silicide source remains on the sample surface, the iron concentration relaxes to that source. This is confirmed by experiments using sources on both sides of the wafers. When the source remains on one side, there is insufficient driving force for the formation of other silicide phases (at the bulk or the other surface), even with a supersaturation of ~2000 times. The supersaturated iron concentration decays substantially more slowly when the iron silicide source has been removed. There is therefore a substantial thermodynamic barrier to nucleation of iron silicide phases at surfaces. It is possible to explain the relaxation kinetics in source-free samples by iron-containing precipitate formation at bulk voids.

ACKNOWLEDGMENTS

The authors are grateful to Radka Chakalova for assistance with sample cleaning and surface passivation. J.D.M. holds a Royal Academy of Engineering/EPSRC Research Fellowship and was supported by a Royal Society Research Grant and an EPSRC First Grant (EP/J01768X/1).

[1]K. Graff, *Metal Impurities in Silicon-Device Fabrication* (Springer, 2000).
[2]G. Coletti, P. C. P. Bronsveld, G. Hahn, W. Warta, D. Macdonald, B. Ceccaroli, K. Wambach, N. Le Quang, and J. M. Fernandez, Adv. Funct. Mater. **21**, 879 (2011).
[3]J. R. Davis, A. Rohatgi, R. H. Hopkins, P. D. Blais, P. Rai-Choudhury, J. R. McCormick, and H. C. Mollenkopf, IEEE Trans. Electron Devices **27**, 677 (1980).
[4]A. A. Istratov, H. Hieslmair, and E. R. Weber, Appl. Phys. A **70**, 489 (2000).
[5]S. M. Myers, M. Seibt, and W. Schröter, J. Appl. Phys. **88**, 3795 (2000).
[6]D. Gilles, E. R. Weber, and S. Hahn, Phys. Rev. Lett. **64**, 196 (1990).

[7]H. S. Radhakrishnan, C. Ahn, J. Van Hoeymissen, F. Dross, N. Cowern, K. Van Nieuwenhuysen, I. Gordon, R. Mertens, and J. Poortmans, Phys. Status Solidi A **209**, 1866 (2012).
[8]H. Talvitie, V. Vähänissi, A. Haarahiltunen, M. Yli-Koski, and H. Savin, J. Appl. Phys. **109**, 093505 (2011).
[9]S. P. Phang and D. Macdonald, J. Appl. Phys. **109**, 073521 (2011).
[10]D. Abdelbarey, V. Kveder, W. Schröter, and M. Seibt, Appl. Phys. Lett. **94**, 061912 (2009).
[11]M. I. Bertoni, D. P. Fenning, M. Rinio, V. Rose, M. Holt, J. Maser, and T. Buonassisi, Energy Environ. Sci. **4**, 4252 (2011).
[12]A. Liu, D. Walter, S. P. Phang, and D. Macdonald, IEEE J. Photovoltaics **2**, 479 (2012).
[13]D. P. Fenning, J. Hofstetter, M. I. Bertoni, S. Hudelson, M. Rinio, J. F. Lelièvre, B. Lai, C. del Cañizo, and T. Buonassisi, Appl. Phys. Lett. **98**, 162103 (2011).
[14]A. A. Istratov, H. Hieslmair, and E. R. Weber, Appl. Phys. A **69**, 13 (1999).
[15]S. A. McHugo, R. J. McDonald, A. R. Smith, D. L. Hurley, and E. R. Weber, Appl. Phys. Lett. **73**, 1424 (1998).
[16]M. B. Shabani, Y. Shiina, S. Shimanuki, and F. G. Kirscht, Solid State Phenom. **82–84**, 331 (2002).
[17]M. Aoki, A. Hara, and A. Ohsawa, J. Appl. Phys. **72**, 895 (1992).
[18]R. Falster and G. Borionetti, in *Recombination Lifetime Measurements in Silicon*, edited by D. C. Gupta, F. R. Bacher, and W. M. Hughes (American Society for Testing and Materials STP, 1998), Vol. 1340, p. 226.
[19]J. D. Murphy and R. J. Falster, Phys. Status Solidi (RRL) **5**, 370 (2011).
[20]D. A. Ramappa and W. B. Henley, J. Electrochem. Soc. **144**, 4353 (1997).
[21]G. Zoth and W. Bergholz, J. Appl. Phys. **67**, 6764 (1990).
[22]W. Wijaranakula, J. Electrochem. Soc. **140**, 275 (1993).
[23]J. Hofstetter, D. P. Fenning, M. I. Bertoni, J. F. Lelièvre, C. del Cañizo, and T. Buonassisi, Prog. Photovoltaics **19**, 487 (2011).
[24]J. Hofstetter, D. P. Fenning, J. F. Lelièvre, C. del Cañizo, and T. Buonassisi, Phys. Status Solidi A **209**, 1861 (2012).
[25]R. Krain, S. Herlufsen, and J. Schmidt, Appl. Phys. Lett. **93**, 152108 (2008).
[26]K. J. Fraser, R. J. Falster, and P. R. Wilshaw, Mater. Sci. Eng., B **159–160**, 194 (2009).
[27]M. Rinio, A. Yodyunyong, S. Keipert-Colberg, Y. P. B. Mouafi, D. Borchert, and A. Montesdeoca-Santana, Prog. Photovoltaics **19**, 165 (2011).
[28]R. A. Sinton and A. Cuevas, Appl. Phys. Lett. **69**, 2510 (1996).
[29]K. Bothe and J. Schmidt, J. Appl. Phys. **99**, 013701 (2006).
[30]D. H. Macdonald, L. J. Geerligs, and A. Azzizi, J. Appl. Phys. **95**, 1021 (2004).
[31]S. Rein and S. W. Glunz, J. Appl. Phys. **98**, 113711 (2005).
[32]J. D. Murphy, K. Bothe, M. Olmo, V. V. Voronkov, and R. J. Falster, J. Appl. Phys. **110**, 053713 (2011).
[33]R. N. Hall, Phys. Rev. **87**, 387 (1952).
[34]W. Shockley and W. T. Read, Phys. Rev. **87**, 835 (1952).
[35]P. G. Shewmon, *Diffusion in Solids* (McGraw-Hill, New York, 1963).
[36]C. S. Fuller and R. A. Logan, J. Appl. Phys. **28**, 1427 (1957).
[37]E. R. Weber, Appl. Phys. A **30**, 1 (1983).
[38]V. Raineri, P. G. Fallica, G. Percolla, A. Battaglia, M. Barbagallo, and S. U. Campisano, J. Appl. Phys. **78**, 3727 (1995).
[39]A. G. Cullis and L. E. Katz, Philos. Mag. **30**, 1419 (1974).
[40]K. Honda, A. Ohsawa, and T. Nakanishi, J. Electrochem. Soc. **142**, 3486 (1995).
[41]E. Nes and J. Washburn, J. Appl. Phys. **42**, 3562 (1971).